Article **Journal Renewable Energy**
December, 2021 Vol.5 No.15 6-22

Thermal evaluation of an indirect air heating system using solar collectors

Evaluación térmica de un sistema de calentamiento indirecto de aire mediante captadores solares

CABRERA-CHAIREZ, Jeisell Marisol†, ORTÍZ-RODRÍGUEZ, Néstor Manuel, VILLEGAS-MARTÍNEZ, Rodrigo Cervando and GARCÍA-GONZÁLEZ, Juan Manuel*

Universidad Autónoma de Zacatecas, Unidad Académica de Ciencias Químicas

ID 1st Author: *Jeisell Marisol, Cabrera-Chairez* / **ORC ID**: 0000.0001.9519.8977

ID 1st Co-author: *Néstor Manuel, Ortíz-Rodríguez* / **ORC ID**: 0000-0002-2202-6776, **CVU CONACYT ID**: 326880

ID 2nd Co-author: *Rodrigo Cervando, Villegas-Martínez* / **ORC ID**: 0000-0003-0474-6734

ID 3rd Co-author: *Juan Manuel, García-González* / **ORC ID**: 0000-0001-7259-5021, **CVU CONACYT ID**: 346241

DOI: 10.35429/JRE.2021.15.5.6.22 Received March 30, 2021; Accepted June 30, 2021

Abstract

One of the current problems is the use of energy obtained from fossil fuels, especially due to the emission of greenhouse gases. An option to replace fossil fuels is the use of alternative energies such as solar or wind energy. The objective of this work is to carry out a thermal and energy analysis of an indirect air heating system that receives energy through solar collectors that operate with water as the thermal fluid used in a food dehydration system, in order to know the efficiency of the system and therefore, make improvements to the circuit, in addition to the characterization of the water storage tank of the system, obtain the amount of energy that can be provided and the behavior of temperatures at different operating flows. According to the methodology, the temperature profile was obtained inside the hot water tank in two modes of operation (heating and energy extraction) reaching temperatures of 50 to 70 ° C, where the optimum temperature for drying is found and in turn reaching an efficiency 84%, compared to a conventional drying system that uses LP gas.

Solar collectors, Dehydration, Alternative energies

Resumen

Una de la problemática actual es el uso de energías obtenida por combustible fósiles, sobre todo por la emisión de gases de efecto invernadero. Una opción para sustitución de los combustibles fósiles es el uso de las energías alternas como pueden ser la energía solar o eólica. El objetivo de este trabajo es realizar un análisis térmico y energético a un sistema de calentamiento indirecto de aire que recibe energía mediante captadores solares que operan con agua como fluido térmico empleado en un sistema de deshidratado de alimentos, para así conocer la eficiencia del sistema y por lo tanto realizar mejoras al circuito, además de la caracterización del termotanque de almacenamiento de agua del sistema, obtener la cantidad de energía que se puede aportar y el comportamiento de las temperaturas a diferentes flujos de operación. De acuerdo a la metodología se obtuvo el perfil de temperaturas dentro del termotanque a dos modos de operación (calentamiento y extracción de energía) alcanzando temperaturas de 50 a 70 °C, donde se encuentra la temperatura óptima para el secado y a su vez alcanzando una eficiencia del 84%, en comparación a un sistema de secado convencional que utiliza gas LP.

Captadores solares, Deshidratación, Energías alternas

Citation: CABRERA-CHAIREZ, Jeisell Marisol, ORTÍZ-RODRÍGUEZ, Néstor Manuel, VILLEGAS-MARTÍNEZ, Rodrigo Cervando and GARCÍA-GONZÁLEZ, Juan Manuel. Thermal evaluation of an indirect air heating system using solar collectors. Journal Renewable Energy. 2021. 5-15: 6-22

*Correspondence to Author (e-mail: jmgarcia@uaz.edu.mx)
† Researcher contributing as first author.

Introduction

Solar drying has a positive impact on the environment and is practically "free", however a disadvantage of solar drying is that solar energy, when used as the sole source of energy for drying, is not always available. Such is the case of a thermosolar pilot plant where the required heat is supplied by two energy sources: solar and liquefied petroleum gas. The use of the solar resource can be achieved through two systems: a direct air heating system and an indirect air heating system. One of the most relevant objectives of this research focused on the thermal analysis inside the thermal storage system in order to take advantage of the energy that such a system provides and thus propose improvements to the system.

Cisneros *et al* (2021), carried out the evaluation of the technical-economic feasibility of the production of electricity from concentrated solar thermal plants, similar to those in this study. Barrantes (2021), analyzed the energy demand both to produce hot water and to cool the different environments of the Clinic of Stomatology of the Señor de Sipan University, by means of an aerothermal pump. Chira *et al* (2020), made the comparison between solar collection systems for the design and analysis of a conditioning system for an office floor. Marchena *et al*. (2021), and Camayo et al. (2021), designed a solar dryer using solar collectors similar to those in this work.

Theoretical framework

To carry out the energy analysis of the indirect air heating system, temperature data, mass flow of the fluids (air and water) in different spaces, the relative humidity of the air and the ener gy inputs (solar and electrical) are used. The mass flow of air is determined by the following expression:

$$\dot{m}_{air} = \rho_{air}\, v_{air}\, A_{c-s} \quad (1)$$

Where: $\boldsymbol{v_{air}}$ is the average air velocity in the duct, $\boldsymbol{A_{c-s}}$ is the cross-sectional area of the duct and $\boldsymbol{\rho_{air}}$ is the air density.

The operation of the indirect air heating system involves incident solar energy and electrical consumption (pumps and fans).

The incident solar energy in the plane of the solar collector in a period of time is evaluated by means of the following expression:

$$E_{inc} = A_C\, \Delta t \sum_{i=1}^{N} I_i \quad (2)$$

Where: A_C is the opening area of the solar collectors, I is the solar irradiance in the collector plane, Δt is the time interval of each measurement and N is the number of measurements made. The electrical energy ($\boldsymbol{E_{elec}}$) consumed in a period of time by the motors (asynchronous three-phase) coupled to the auxiliary equipment is determined by:

$$E_{elec} = \sqrt{3} \cdot A \cdot V \cdot PF \cdot t_{op} \quad (3)$$

Where: A is the electrical current, V is the electrical voltage, PF is the power factor and $t_{op}$is the operating time of the fan or pump. The instantaneous useful energy transferred to a thermal fluid is determined by the following expression:

$$\dot{Q}_u = \dot{m}\, Cp_{mf}\, \left(T_{f,out} - T_{f,in}\right) \quad (4)$$

While, the useful energy transferred to a thermal fluid in a period of time (accumulated) is determined by the equation:

$$E_u = \Delta t \sum_{i=1}^{N} \left[\dot{m}\, Cp_{mf}\, \left(T_{f,out} - T_{f,in}\right)\right]_i \quad (5)$$

Where: $\dot{m}$ is the mass flow of the thermal fluid, Cp_{m_f} is the average heat capacity at constant pressure of the thermal fluid, $T_{f,in}$ and $T_{f,out}$ are the inlet temperatures and thermal fluid outlet, respectively. Not all the energy available from the solar resource is transferred to the hot air that enters the drying chamber. The initial energy is lost sequentially through the different components that make up the overall drying system. Part of the energy from the solar resource is lost through solar collectors. The instantaneous thermal efficiency of the solar collector field is defined as the relationship between the gain of useful energy by the thermal fluid and the incident solar energy, at a given instant, by means of the expression (García *et al*., 2019):

$$\eta_{t,c} = \frac{\dot{m}\, Cp_{mf}\, \left(T_{f,out} - T_{f,in}\right)}{I\, A_C} \quad (6)$$

ISSN 2523-2881

The global energy efficiency of solar energy collection systems considering the electrical energy consumption of auxiliary equipment (E_{elec}) is determined by the following expression (García *et al.*, 2020):

$$\eta_{g,e} = \frac{E_{u,\ agua}}{E_{inc}+E_{elec}} \quad (7)$$

Part of the useful energy gained in solar water heaters is stored in the hot water tank during the heating operation. Therefore, the water contained in the hot water tank increases its temperature and, therefore, its thermal energy. The overall thermal efficiency of the water heating system can be defined as the ratio between the thermal energy gained by the tank and the total incident solar energy during effective operation (water pumps on):

$$\eta_{t,S.C.A} = \frac{E_{tanque}}{E_{inc}} = \frac{[m_T\ Cp_m\ (T_{final}-T_{inicial})]_{Agua\ tanque}}{E_{inc}} \quad 8)$$

Solar water heaters are not the only heat exchangers in the indirect air heating system. Also, it is made up of plate and finned tube heat exchangers. In a heat exchanger with two fluids in between, the fluid with a higher temperature (subscript h) gives up part of its heat to the fluid with a lower temperature (subscript c) and there are also some losses to the environment.

Therefore, a parameter of interest to be determined in a heat exchanger is the instantaneous thermal efficiency of heat transfer. Which can be defined by the following expression:

$$\eta_{int} = \frac{\dot{Q}_c}{\dot{Q}_h} = \frac{\dot{m}_c\ Cp_{mfc}\ (T_{fc,out}-T_{fc,in})}{\dot{m}_h\ Cp_{mfh}\ (T_{fh,out}-T_{fh,in})} \quad (9)$$

Also, it is possible to determine the global thermal efficiency of the heat transfer during the total interval of operation of the exchanger, by means of the expression:

$$\eta_{int} = \frac{E_{u,c}}{E_{u,h}} = \frac{\Delta t \sum_{i=1}^{N}[\dot{m}_c\ Cp_{mfc}\ (T_{fc,out}-T_{fc,in})]_i}{\Delta t \sum_{i=1}^{N}[\dot{m}_h\ Cp_{mfh}\ (T_{fh,out}-T_{fh,in})]_i} \quad (10)$$

Equipment and materials

Solar energy drying systems are broadly classified into two large groups: active systems (forced convection) and passive systems (natural convection).

Three different subclasses of active or passive solar drying systems can be identified (which vary mainly in the design arrangement of the system components and the way in which solar heat is used): distributed, integral and mixed type solar dryers (Ekechukwu & Norton, 1997). Distributed mode is one in which the solar collector and the drying chamber are separate units. While the integral solar energy harvesting unit is an integral part of the entire system, so there is no need for a special duct to channel the drying air to a separate drying chamber. Mixed mode combines some features of the distributed and integral types (Ekechukwu & Norton, 1999).

The pilot drying plant in the state of Zacatecas was designed with a hybrid solar drying system distributed by forced convection. This system is basically made up of: A dehydration chamber, 40 solar thermal energy collectors, conventional heat backup, thermal storage and auxiliary equipment.

Solar collectors based on a liquid thermal fluid can be used indirectly by using a liquid-gas heat exchanger to heat the hot air required for drying food. The plant's indirect air heating system is made up of: A field of flat solar collectors for heating water, a liquid-liquid plate heat exchanger. A hot water tank, a water-air finned tube heat exchanger, a centrifugal fan and auxiliary equipment (water pumps, expansion vessel, valves and air eliminators).

The field of solar collectors for indirect air heating is made up of 40 MAXOL MS2.5® collectors, equivalent to a collection area of 92.44 m^2, distributed in four banks (rows) in parallel, each one made up of two arrangements of five collectors in parallel connected in series (10 collectors per row).

This type of collectors has an aluminum absorber plate and a network of 11 copper tubes (risers). The absorbing surface has a selective titanium oxide coating to increase the ability to absorb solar radiation. The collectors are covered with low iron 4mm textured tempered solar glass. The side walls and the bottom of the collector are insulated with polyurethane and mineral wool. The frame that supports the collector components is made of rolled steel. The effective area of each collector is 2.32 m^2.

ISSN 2523-2881

In Figure 1, you can see the key equipment that makes up the indirect air heating system; as well as its instrumentation (Ortíz *et al.,* 2020). The solar collectors of the water heating system are oriented to the Equator with an inclination of 22.72 ± 0.94 (which is practically the same as the geographical latitude of the location of the plant φ = 22.89°) and with a separation between row of 92 cm. Figure 2 schematically presents the arrangement of the flat solar collector field for water heating, as well as the location of the sensors that record the variables of interest.

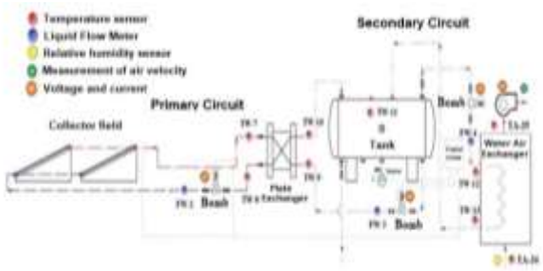

Figure 1 Instrumentation of the indirect air heating system

.

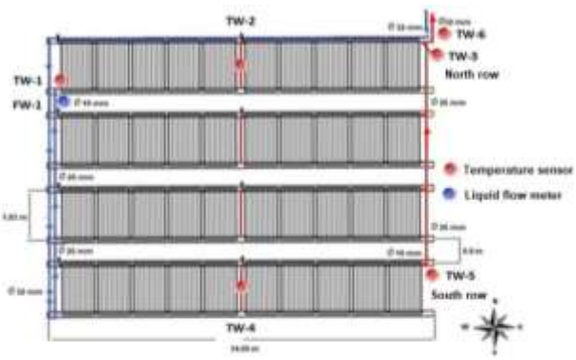

Figure 2 Arrangement of solar collectors for water heating

Operation mode

Hot water from water-based solar collector systems can be used directly in the water-air heat exchanger (DIRECT MODE) or stored in a thermal tank for later use (STORAGE MODE).

The solar collector system for water heating operates by a forced circulation system made up of a closed primary circuit and an open secondary circuit. Both circuits contain treated water less than 50 ppm of hardness to avoid the incrustation of salts in the equipment. Each circuit operates with a 1.5 hp (745.7W) pump with a nominal flow rate of up to 160 l / min. The primary circuit is responsible for removing the useful heat from the solar collector field by recirculating the water.

Meanwhile, the secondary circuit is in charge of transporting the useful heat for direct use or storage.

The primary circuit has an inverted return pipe that allows the paths of the working fluid to equalize, favoring hydraulic balance and reducing pressure losses. The pipes of the primary circuit are made of copper, while those of the secondary circuit are made of polypropylene (random copolymer). It should be noted that only the primary circuit has fiberglass insulation covered with aluminum foil. In addition, said circuit has an expander vessel (325.5 liter volume) that allows the collector field to remain stagnant without the need to release liquid to reduce the pressure in the circuit.

The useful heat that comes from the solar collector field is transferred from the primary circuit to the secondary circuit by means of a plate heat exchanger (10 ribbed stainless steel plates). The hot water that comes out of the plate exchanger and is transported by the secondary circuit can be used directly or stored in the thermo tank. It also has a water-air heat exchanger that allows the indirect heating of the air through the energy that is captured by the solar heating system.

The exchanger consists of a finned tube system with 125 tubes of 38” long (965.2mm) and 5/8" outside diameter (15.875 mm) and with circular aluminum fins with a fin diameter of 1 ½" (38.1 mm), with 10 fins per inch (394 fins / m). The hot water flows into the tubes and the air flows outside the finned tubes, gaining the sensible heat given off by the hot water.

The air flow to be heated for drying is provided by a centrifugal fan coupled to a 10 hp motor. (Maximum BHP: 30 and Maximum rpm: 1300). The centrifugal fan sucks the air out of the water-air exchanger, therefore, it operates at negative pressure in that section. The fan has a frequency variator that allows to regulate the air flow required at the inlet of the drying chamber. The ease of variation in the volume and temperature of the air in the drying chamber easily allows the possibility of treating food products of various kinds.

ISSN 2523-2881

The thermal storage tank acts as a heat accumulator and backup for the drying system. Thermal storage makes it possible to have more uniform temperatures in the heat exchanger than the hot water coming directly from the solar collectors, as well as to have thermal energy available at night and during periods with adverse weather conditions (very cloudy and rainy days). They also have a horizontal atmospheric tank with a capacity of 6,450 liters for storing hot water. The tank is filled with 6,150 liters, to cushion the volume changes of the water due to the increase in temperature. The tank is made of carbon steel with epoxy coating on the inside and on the outside it has a thermal insulation of fiberglass of 2 pulgadas (50.8 mm) with an aluminum foil cover.

In storage mode, the system has a differential temperature control that activates the primary and secondary circuit pumps when the difference between the temperature of the working fluid at the outlet of the collector field and the water temperature in the lower part of the tank exceeds a set value of 8 °C. When the temperature difference falls below 4 °C the pumps are deactivated. In addition, the control is programmed to stop the pumps when the tank reaches a temperature of 90 °C, this limit is the maximum operating temperature of the water pumps.

When the indirect air heating system is operated in storage mode, there is a tertiary circuit. This is in charge of extracting the energy from the tank and delivering it to the finned tube exchanger. For this, there is a ¾ hp (559.275W) water pump with a nominal capacity of up to 90 l / min, which is used to transport the hot water to the water-air heat exchanger. The water that comes out of the exchanger is recirculated in the central part of the tank. The pump is connected to a frequency variator that allows regulating the flow of hot water that passes through the exchanger.

The operating variables of the components that make up the dewatering system of the pilot plant are recorded simultaneously using data loggers and an automated data acquisition system, with the exception of air pressure differentials and velocities, which are recorded manually. Measurements are recorded using two Agilent Model 34970A data loggers, with three digital multiplexers of 22 channels each and one analog multiplexer.

The latter is used exclusively for the weather station. Data acquisition and recording was scheduled in one minute. Relative humidity was measured with Iberian sensors. The volumetric flow of water was measured with magnetic paddle sensors that send a frequency signal. Temperatures were measured with calibrated 3-wire RTD sensors, protected with reflective stainless steel cylinders; the connection to the data logger was made in two wires. An adjustment was made to the signal delivered by the sensor, due to the additional resistance due to the long distances between the sensors and the logger. A hot wire anemometer was used to measure the air flow velocity in the air discharge duct of the finned tube heat exchanger.

It has a meteorological station made up of: a Kipp & Zonen CM3 pyranometer to measure horizontal solar irradiance, a Davis 6410 cup anemometer to measure the horizontal component of wind speed and its direction, a Davis model 7852 rain gauge to measure the rain precipitation and an Iberian sensor model PCE-P18 for the measurement of relative humidity and ambient temperature. The meteorological station is installed at a height of eight meters from the floor of the plant, avoiding the interference of the exhaust gases from the drying chamber and shading effects.

The water heating monitoring system is made up of the primary circuit consisting of eight temperature sensors, two flowmeters: one to measure the global flow to the collector field and the other to measure the flow of the North row of the collector field. The secondary circuit has two temperature sensors in the plate exchanger and a flow meter. A Kipp & Zonen CMP3 pyranometer was installed on the solar water collectors to measure the solar irradiance in the inclined plane. The distribution of the sensors makes it possible to determine the overall efficiency of the collector field, as well as the efficiency of the exchange system between both circuits, see Figure 1, and Figure 2. The water-air heat exchanger consists of four temperature sensors and a flow meter, which allow the efficiency of the exchanger to be determined. The thermal storage tank has a temperature sensor, additionally it has a bimetallic dial thermometer in the middle. In Figure 3, you can see the distribution of some of the sensors used to monitor the variables of interest (Ortíz *et al.*, 2021).

ISSN 2523-2881

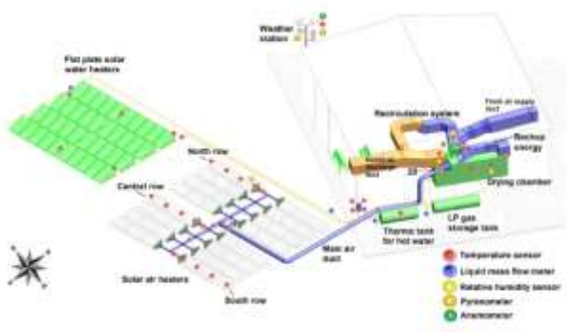

Figure 3 Schematic representation of the distribution of some of the sensors installed in the plant

The installation of temperature sensors at different levels inside the tank was carried out as illustrated in Figure 4 to observe how the behavior is inside and carry out the energy analysis of the same. Wireless capsule type sensors (DST-milli-TD) were used that serve to record the temperature of small depth (Figure 5).

They are ideal for placement in different aquatic conditions, with dimensions of 39.4 mm x 13 mm, with a protective plastic shell to be able to submerge. It also has a large memory capacity, with 699,000 temperature measurements in a standard temperature range of -1 °C to + 95 °C.

They have a communication box in which you are given the instructions to activate the capsules and deactivate them, how to measure, the measurement time as well as obtaining the data after performing the measurement tests (Hauer, 2007).

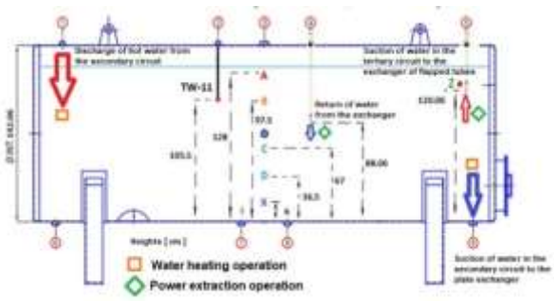

Figure 4 Instrumentation inside the energy storage tank

For the installation of the capsules inside the tank, a carbon steel wire was used as a support. In which the capsules were held, at different distances, with the help of a heat shrink tube which, when heated to 70 °C, shrinks to 50% of its original size.

Figure 5 DST-milli-TD temperature recording capsules (Hauer, 2007)

Results and Discussion

Table 1 shows the meteorological parameters recorded during the experimentation. On average, a difference between the maximum and minimum values of ambient temperature of ≈ 20 °C was recorded, which reflects a large temperature range between day and night, which is a characteristic of the region's semi-desert climate, especially the winter months. Another characteristic of the environmental conditions of the region and the season is the low relative humidity of the air. For the tests, an average minimum ambient relative humidity of ≈ 15% was recorded.

Parameters	Heating		Extraction	
	Average	Standard Deviation	Average	Standard Deviation
Average ambient temperature * (°C)	8.79	1.5	10.47	0
Maximum ambient temperature * (°C)	19.375	3.595	23.62	2.46
Minimum ambient temperature* (°C)	-0.465	0.445	1.01	1.71
Average ambient relative humidity * (%)	24.985	3.215	48.03	0
Maximum ambient relative humidity * (%)	38.63	1.94	71.575	8.565
Minimum ambient relative humidity * (%)	12.345	4.225	14.8	4
Average ambient temperatura** (°C)	13.805	2.165	16.19	0
Minimum ambient temperature** (°C)	1.555	0.265	3.375	3.215
Average ambient relative humidity ** (%)	20.34	3.13	29.085	7.955
Maximum ambient relative humidity ** (%)	35.84	0.16	69.205	10.805
Average ambient temperature***(°C)	17.76	3.35	16.45	3.03
Maximum ambient temperature***(°C)	19.375	3.595	21.205	3.055
Minimum ambient temperature***(°C)	13.595	2.195	12.105	2.315
Average ambient relative humidity *** (%)	15.785	3.885	20.32	6.81
Maximum ambient relative humidity *** (%)	22.775	2.645	24.935	7.635
Sun hours (h)	10.6	0	11.035	0.345
Global irradiance on the average collector surface** (W/m^2)	648.36	25.9	658.51	0
Global maximum irradiance on the collector surface **(W/m^2)	1084.43	4.46	1068.96	0
Total daily irradiation on the collector surface ** (MJ/m^2)	26.975	0.165	26.04	0
Total daily irradiation in horizontal plane** (MJ/ m^2)	18.115	0.025	18.05	0

* Registered 24 hours a day
** Recorded during sunny hours
*** Recorded during actual heating and extraction operation

Table 1 Meteorological parameters recorded during the experimentation

The heating tests were carried out with half of the catchment area of the water heaters (north and south row, since the others were disconnected due to leaks). Because of this, there is a higher flow per row, although the overall flow is similar to the normal four-row configuration operation.

Before performing the energy analysis of the components of the heating system, an analysis of the mass flows involved was carried out: flow of the north row (FW-1), global flow of the primary circuit (FW-2) and global flow of the secondary circuit (FW-3).

The registered data of the FW-2 flow were considered to obtain a proportional relationship with the FW-1 flow, in order to be able to estimate the FW-2 flow in the intervals in which there are no records. Meanwhile, for the case of the FW-3 flow, the average of the data recorded for said flow was considered. When tests have been carried out with four rows of collectors, a ratio of 0.221 (FW-1/FW-2) has been obtained.

This parameter was used to correct and estimate a relationship with two rows of collectors. The analysis for two rows yielded a value of 0.4419 (FW-1 / FW-2) and it was used, together with the registered FW-1 data, to estimate the global mass flow of the primary circuit (FW-2) and of the south row. Table 2 shows the data of the mass flows of the primary circuit (north row flow (FW-1), south row and global circuit flow (FW-2). The south row flow was calculated as the difference between the global flow and the flow of the north row.

Parameter	By pass-open			By pass-closed		
	FW-1	FW-2	Row south	FW-1	FW-2	Row south
Maximum	43.77	99.04	55.27	39.78	90.00	50.23
Minimu	41.37	93.60	52.24	36.95	83.61	46.66
Average	42.32	95.76	53.44	38.46	87.03	48.57
Standard deviation	0.53	1.19	0.66	0.46	1.04	0.58

Table 2 Measured and estimated flows of the primary circuit

From these data, the energy analysis of three of the key components of the heating system was carried out: solar collectors, plate heat exchanger and storage tank. For both tests, the volume of water contained in the tank was 6150 l.

The water heating system was left in automatic mode by means of a differential control with the following parameters: switch-on difference 8 °C, switch-off difference 4 °C and maximum switch-off temperature 90 °C. The results obtained are presented below.

The temperature inside the tank was 26.79 °C. There was an effective test period of 5.5 continuous hours in which the average global irradiance on the collector plane was 948.15 W / m2. During the operating period the temperature of the water stored in the tank increased to 44.10 °C. In Figure 6, the temperature profile is presented: at the entrance (TW-1) and at the exit (TW-6) of the solar collector field, as well as the temperature progression in the thermo tank (TW-11) and ambient temperature. The solar irradiance is also presented in the plane of the collector and it can be seen that it was a totally clear day.

In Figure 7, the instantaneous efficiencies of the north, south and global row of the field of solar energy collectors for water heating are presented; as well as the useful energy delivered by the solar collectors and the energy accumulated in the hot water tank.

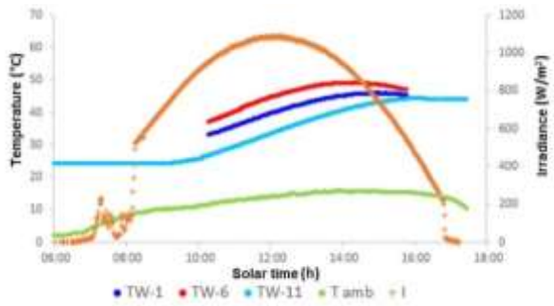

Figure 6 Temperature profile in the field of solar collectors for water heating, hot water tank and solar irradiance

Instantaneous thermal efficiency was determined by equation (6). The area used to determine the efficiency of both rows was 23.11 m2; while for the global it was 46.22 m2. The average heat capacity was 4179 J / kg K in a temperature range of 33.02 ° C to 46.79 ° C for the water in the collectors, as well as the average heat capacity was 4178.97 J / kg K in a temperature range of 26.21 ° to 43.65 ° C for the water in the tank.

ISSN 2523-2881

It can be seen that the instantaneous efficiencies of the north row are relatively lower than those of the south row and the global ones, this is due to the lower mass flow compared to the flow of the south row and the global flow of the primary circuit of the field of solar collectors. During the 5.5 hours of testing, the total incident energy on the 20 solar collectors was 867.7 MJ, while the useful energy removed by the water was 489.28 MJ. Therefore, the global thermal efficiency of the solar collector field was 54.44%. At the end of the test, the energy contained in the tank water was 448.19 MJ. Therefore, 8% of the useful energy is lost during the transport and storage of hot water to the tank.

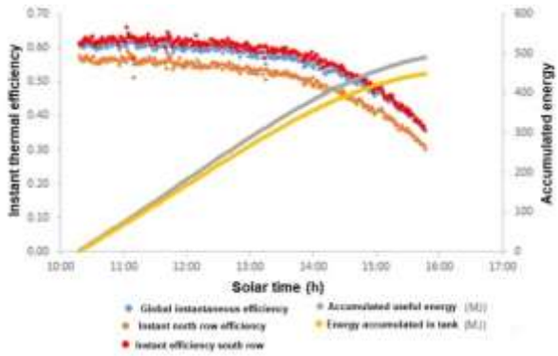

Figure 7 Instantaneous thermal efficiencies and accumulated energ

Another important component in the water heating system is the plate exchanger, this was evaluated by determining its thermal efficiency through equation (9). In Figure 8, the thermal efficiencies of the plate exchanger are presented. As can be seen, the criterion of having an efficiency lower than one around 0.6 is met, which means that in the exchange there are losses to the environment. These results were to be expected because the flows recorded in the secondary circuit (FW-3), during these tests, were low compared to the previous tests (greater than 60 kg/min).

Therefore, the results of the plate heat exchanger efficiencies are not correct. However, a thermal analysis can be performed with the temperatures obtained during the tests. In Figure 8, the behavior of the quotient between the increase in water temperature on the side of the secondary circuit is presented ($T_{fc,out} - T_{fc,in}$) and the decrease in water temperature on the side of the primary circuit $\left(T_{fh,out} - T_{fh,in}\right)$.

Despite not having the correct mass flow that passes through the secondary circuit (FW-3), it is expected that the mass flow and heat capacity in both circuits (FW-2 and FW-3) are constant practitioners. Therefore, the efficiency of the exchanger would only be a function of the quotient between the temperature differential of both circuits. Therefore, observing the behavior of the quotient (see Figure 8), it is expected that the efficiency increases during the test period. However, as the heating proceeds, the temperatures increase.

The greatest heat losses are generated as the temperature increases with respect to that of the environment. Taking this into account, the result seems a bit contradictory. However, it must be borne in mind that it is not a stable process and in the first hours of startup it is to be expected that there will be greater losses due to the preheating of the thermal inertia of the equipment. This behavior of the quotient is also similar to the results of previous tests with the complete solar collector field.

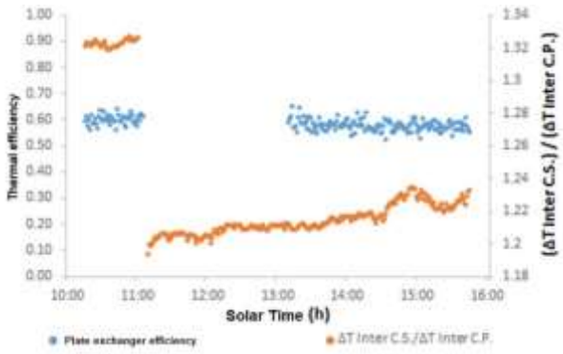

Figure 8 Thermal efficiencies and quotient between the plate heat exchanger temperature differentials

To appreciate the temperature distribution inside the water storage tank, four wireless capsule-type sensors were installed at different heights with respect to the bottom of the tank, as shown in Figure 9. In addition to the capsule-type sensors, there are also The sensor is a PT-1000 (TW-11) sensor that normally records the temperature of the thermo tank through the data logger.

In Figure 10, the water temperature profiles are presented at the different heights inside the tank. Despite the fact that during heating there is agitation inside the tank due to the suction (point 9, Figure 9) and discharge (point 1, Figure 9) of water from the secondary circuit, it can be observed that there is a slight stratification of the temperatures.

ISSN 2523-2881

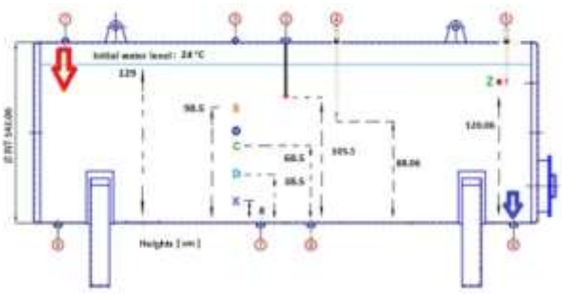

Figure 9 Distribution of the temperature sensors inside the hot water tank

As expected the highest temperatures are at the top of the tank and vice versa. The average difference between the upper temperature (TW-11) and the lower one (X) was 0.9 ° C and with a maximum close to solar noon of 1.24 ° C. These differences are very small and practically indicate that the horizontal tank does not allow a significant stratification of the temperature in its interior (see Figure 10).

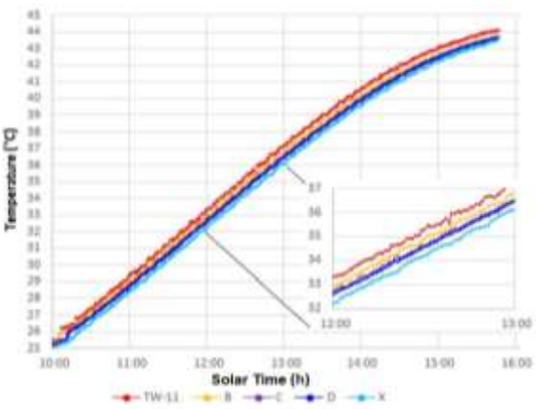

Figure 10 Stratification of temperatures in the tank of December 20

In the literature, the analysis of stratification using 2D graphics is common, representing the temperature on an axis of the abscissa and the height of the water level in the storage tank on the axis of the ordinate. In Figure 11, the distribution of the water temperatures inside the tank at different times during heating is presented. In these types of graphs, a vertical line means that the temperature of the water inside the tank is uniform, that is, that the water in the tank is completely mixed. As previously discussed, the degree of stratification is low during heating. Therefore, it is to be expected that the performance of the solar collector system will be low as has been reported in other investigations.

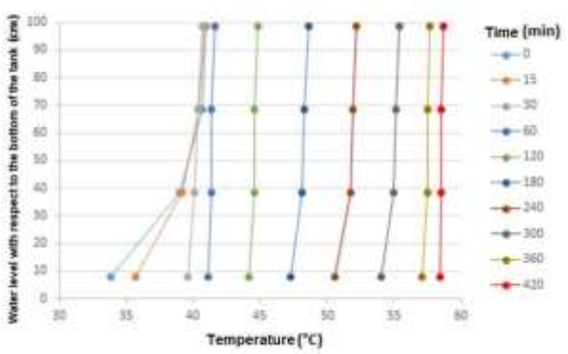

Figure 11 Evolution of the temperature profiles inside the tank.

In order to evaluate the behavior of the indirect air heating system, two ways of extracting the energy stored in the thermal tank were tested: maximum flow and varied flow of water through the water-air heat exchanger. For the maximum flow test, the water pump was operated at 60 Hz delivering an average flow of 55 kg/min. For the variable flow test, the flow rate of water passing through the exchanger was regulated between (18-55) kg/min, in such a way that the air temperature at the outlet of the exchanger was kept between 55 and 50 °C.

The energy extraction in the hot water tank ended when the air temperature at the outlet of the exchanger was below 50 °C. In all tests, the water content inside the tank was 6150 liters and the volumetric flow of air through the exchanger was 6367.78 m^3 / h, operating the centrifugal fan at 35 Hz.

For the energy extraction test, five wireless capsule-type sensors were installed inside the hot water tank in order to determine the thermal behavior inside it. These were installed in the central part of the tank at different heights from the bottom of the hot water tank, as shown in Figure 12. In addition to the capsule-type sensors, the PT-1000 (TW-11) sensor was also relocated, which normally records the temperature of the tank, thermotank through the data logger. In Figure 12, you can see the locations and heights in which the water used in the heat exchanger is sucked (position 5) and returned (position 4) to the tank. As can be seen, the water that goes to the exchanger is sucked above ¾ parts of the water level in the tank, while the water that returns from the exchanger is discharged just above the middle.

ISSN 2523-2881

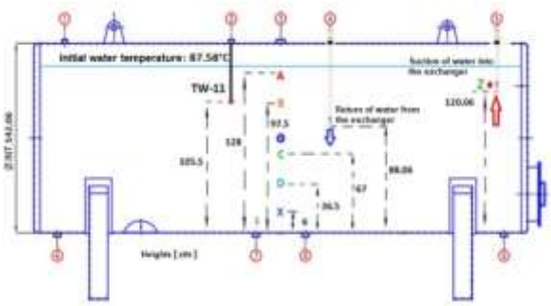

Figure 12 Distribution of the temperature sensors inside the hot water tank

In Figure 13, the variables of interest are presented for the analysis of the energy extraction of the hot water tank. Only the temperature profiles of the capsule type sensors are presented in the highest (A) and lowest (X) position relative to the tank, for a clearer representation of the temperature profiles inside the tank. It can be seen that before the start of the test there is a stable stratification of the temperature inside the tank. Initially, the temperature difference between position A and X was 3.9 ° C. Once the water pump is turned on (55.06 ± 0.51 kg / min) that extracts the energy from the hot water tank, it will be observed that initially stratification persists, however, as the energy extraction operation progresses at maximum flow, the temperatures inside the tank are very similar which indicates practically a complete mixing inside the tank.

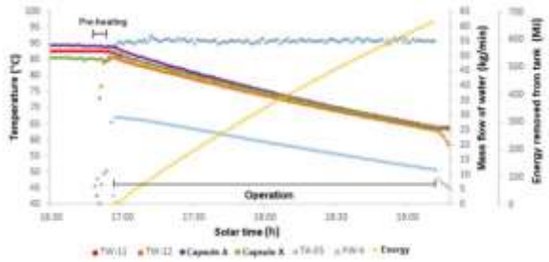

Figure 13 Temperature profiles in the exchanger and in the hot water tank, as well as the mass flow of water through the exchanger during operation

Once the energy extraction operation (hot water) from the tank is finished, the convective movement of the water stops and the temperature stratification inside the tank begins. In Figure 14, the behavior of the water temperature profiles inside the tank can be observed in the highest position (A) and lowest (X) with respect to the bottom of the tank. In addition to the stratification of the temperatures, it is also possible to observe the decrease in temperature (negative slope), in general, of both profiles in the two zones of the tank.

This is due not only to the stratification, but also to the losses of heat to the environment. Before the automatic start of the pumps for heating the water, the maximum difference between the temperature of the upper and lower water inside the tank was 6.78 ° C.

Figure 14 shows the temperature profiles of the water at the inlet (TW-12) and at the outlet (TW-13), of the air at the inlet (TA-34) and at the outlet (TA-35) of the exchanger finned tube heat and instantaneous thermal efficiencies; as well as the mass flow of water. The air temperature at the outlet of the exchanger was kept above 50 °C. The maximum air temperature at the outlet of the exchanger was 67 °C. The instantaneous thermal efficiency of the average exchanger was 0.7414 ± 0.0114.

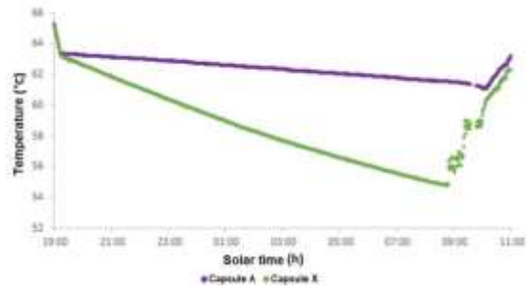

Figure 14 Stratification of temperatures inside the tank during non-operating hours

Using Equation (9), the thermal efficiency of the heat exchanger was determined heat from water-air finned tubes. The flow rate of the air used was considered constant and equal to 6366.78 m^3/h (average density: 0.86414 kg/m^3). The average heat capacity for water was 4187.1 J/kg K and that of humid air was 1008.3 J/kg K (Figure 15).

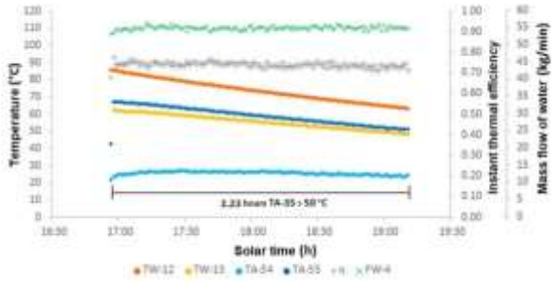

Figure 15 Thermal efficiency and temperature profile of the exchanger at maximum water flow

ISSN 2523-2881

The average temperature of the tank (determined with the five capsule type sensors and TW-11) is reduced from 87.61 °C to 63.8 °C, contributing a total of 616.83 MJ of thermal energy stored in the hot water tank to the indirect heating process of the air. The useful heat delivered to the air in the heat exchanger was 415.73 MJ, therefore, 32.53% of the energy provided by the hot water tank was lost during the indirect heating of the air.

In Figure 16, the accumulated energy profiles are presented during the indirect heating of the air. In which it is possible to observe the energy that is removed from the tank by means of the extraction of hot water and the inherent heat losses of the tank itself, as well as the useful energy that the hot water supplies in the heat exchanger and the energy which is absorbed by the air during heat exchange. 8.8% of the energy removed from the tank is lost during its transport in the pipes to the exchanger and 23.66% is lost in the heat exchanger.

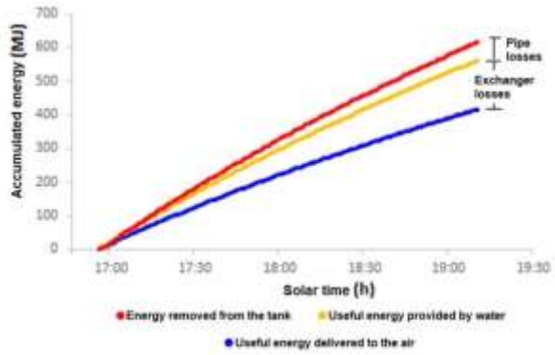

Figure 16 Energy profiles during indirect air heating

During the operation of the indirect heating system with varied flow, the flow rate of the hot water flow that passed through the exchanger was regulated in such a way that the air temperature at the outlet of the exchanger was 53.34 ± 2.21 °C. Table 3 shows the variation of the mass flow during the extraction test. Only four capsule-type sensors and the PT-1000 (TW-11) sensor were available for this energy extraction test. The layout of the sensors inside the hot water tank is schematically presented in (Figure 17).

		Frequency Water Pump (Hz)	Average mass flow of the water (kg/min)	TA-35 (°C)	
16:18	16:28	10	22.5	NA	NA
16:28	18:41	133	22	54.63	54.63
18:41	18:43	2	27	52.40	52.40
18:43	19:17	34	29	52.99	52.99
19:17	19:32	15	35	51.93	51.93
19:32	19:38	6	40	50.11	50.11
19:38	19:42	4	45	49.03	49.03

Table 3 Variation of the mass flow of water during energy extraction

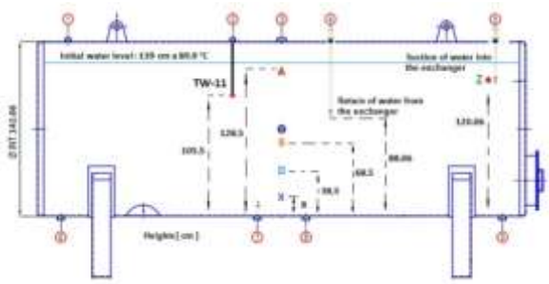

Figure 17 Distribution of the temperature sensors inside the hot water tank

In Figure 18, the parameters of interest for the analysis of the energy extraction of the hot water tank are presented. It can be seen that at 2:00 p.m. the hot water tank had already reached the maximum allowed temperature (90 °C). From 2:40 p.m. to 2:50 p.m., the water pump of the water-air exchanger was turned on, in order to eliminate the air that was initially trapped inside the exchanger tubes (pre-operation). This causes the temperatures recorded by the sensors that record the temperature of the water at the inlet (TW-12) and the air at the outlet (TA-35) of the heat exchanger to increase suddenly.

The energy extraction operation for the indirect heating of the air began with an average flow of 18.8 kg/min and gradually increased in order to maintain the desired air temperature at the outlet of the exchanger. The energy extraction operation ended when the TA-35 was 47.8 °C. During operation, the air temperature at the exit of the exchanger was between 47 and 56 °C and the average air temperature at the entrance of the tunnel was 53.3 ± 2.21 °C.

ISSN 2523-2881

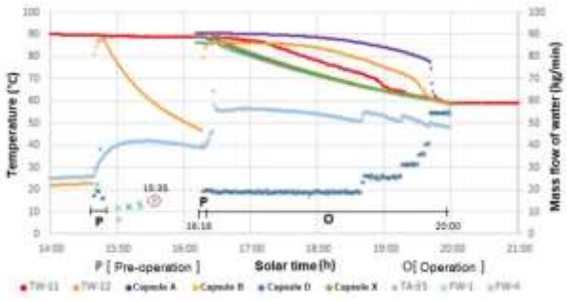

Figure 18 Temperature profiles in the exchanger and the hot water tank, as well as the mass flow of water in the exchanger

In Figure 19, the temperature profiles inside the hot water tank are presented during the energy extraction operation at different water flows through the exchanger. It can be seen that just before the pump is turned on there is a stable temperature gradient between the different sensor positions, which means, the stratification of the water temperature inside the hot water tank. As expected, the highest position is the one with the highest temperature and vice versa. Initially, the temperature difference between position A and X was 4.31 °C. Once the pump is turned on, it can be observed that the stratification persists, however, it is no longer stable due to the mixing that begins to happen inside the tank due to the suction and return of water during the extraction of energy.

In Figure 20, it is observed that at lower flow (18.9 kg/min) mixing is more evident in the positions below the discharge of the return water. As the operation progresses and the water flow increases, mixing at other levels of the water inside the tank begins to be relevant. Increasing the flow up to 25 kg/min causes significant mixing to the TW-11 position and increasing to 31 kg/min until water suction (position Z, the temperature in this position is similar to the water temperature at the inlet of the exchanger, the temperature difference between them is due to heat losses in the pipe). When the maximum flow is reached (54 kg/min), a complete mixing occurs between the different positions registered inside the tank.

Therefore, there is no significant stratification in between the measured positions and the temperatures are practically the same. With these observations it can be concluded that the gradual increase in the flow of the water extraction delays the complete mixing of the tank, which allows to prolong the operation time of the indirect heating of the air with a desired temperature.

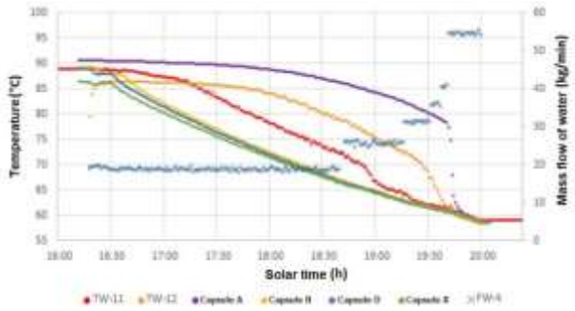

Figure 19 Temperature profiles inside the tank and the mass flow of water in the exchanger

Using Equation (9) the thermal efficiency of the water-air finned tube heat exchanger was determined. The flow of the air used was considered constant and equal to 6366.78 m^3/h (average density: 0.8701 kg/m^3). The average heat capacity for water was 4186 J/kg K and that of humid air was 1003 J/kg K. In Figure 20, the temperature profiles of the water at the inlet (TW-12) and at the outlet are presented. (TW-13), of the air at the inlet (TA-34) and at the outlet (TA-35) of the finned tube heat exchanger and the instantaneous thermal efficiencies; as well as the mass flow of water in the heat exchanger. The air temperature at the outlet of the exchanger was kept above 50 °C when the water flow was less than 40 kg/min. The instantaneous thermal efficiency of the average exchanger was 0.8478 ± 0.0301.

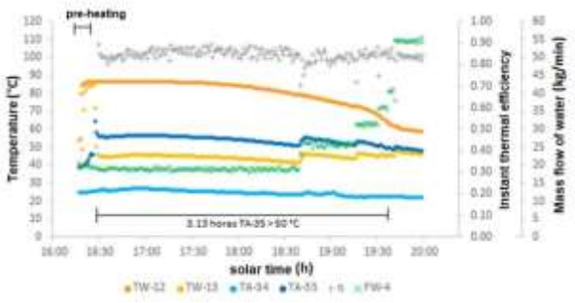

Figure 20 Thermal efficiency and temperature profile of the exchanger when the water flow is varied

The average temperature of the tank (determined with the four capsule type sensors and TW-11) is reduced from 88.27 °C to 58.92 °C, contributing a total of 758.17 MJ of thermal energy stored in the hot water tank to the indirect heating process of the air. The useful heat delivered to the air in the heat exchanger was 576.42 MJ, therefore, 25.22% of the energy removed in the hot water tank was lost during the indirect heating of the air. In Figure 21, you can see the energy removed and the decrease in the average temperature in the hot water tank.

ISSN 2523-2881

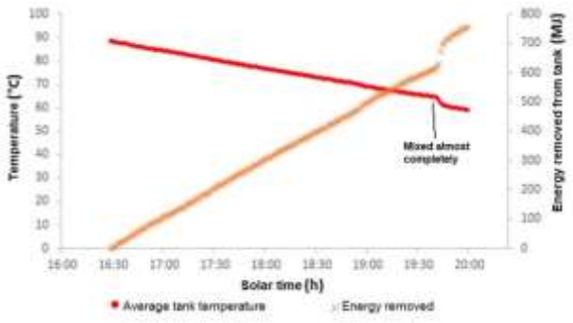

Figure 21 Power extraction during operation

Conclusions

The results of the thermal analysis have demonstrated the technical feasibility of using solar thermal technologies for indirect heating of the air for drying products. The highlights of the work are: The indirect solar air heating system is capable of delivering the required temperature in the food drying process, that is, temperatures between 50 ° C and 70 ° C. The indirect solar heating system of Air in storage mode allows the temperature of the air at the inlet of the drying chamber to be regulated.

The extraction of thermal energy in the hot water tank gradually from a low flow to a maximum flow allows better use of the stored energy and extends the heat supply time around 3.53 hours. A longer heat supply from indirect air heating can minimize the use of L.P. gas heating backup.

During the solar water heating operation and the extraction of thermal energy in storage mode, there is no thermal stratification inside the tank. However, the gradual extraction of energy generated greater stratification than a maximum flow extraction.

The field of water-based solar collectors obtained thermal efficiencies of 52.88%. However, the overall thermal efficiency with respect to the energy delivered to the finned tube heat exchanger decreases in a cascade, since it has several stages to be able to heat the air used in the drying process.

The development and implementation of technology for solar drying systems, initially on a demonstrative scale, in the Mexican industrial sector could allow a technical and economic maturation of the technology, and the benefits could be presented in the short term.

Acknowledgments

This work was supported by FORDECYT Project No. 190603 and SECAMPO Zacatecas.

References

Aguilar Hernández R. y Esparza Frausto G., (2010) «Situación y perspectivas de la producción de chile seco en Zacatecas», *Revista de geografía agrícola*, n.º 45, Art. No. 4, Accedido: sep. 27, 2020. [En línea]. Disponible en: http://www.chapingo .mx/revistas/ geografia/contenido.php?anio=2009&vol=.

Antonanzas T. F., Urraca R., Polo J., Perpiñán-L. O., y Escobar R., (2019) «Clear sky solar irradiance models: A review of seventy models», *Renewable and Sustainable Energy Reviews*, vol. 107, n.º March 2018, pp. 374-387, doi: 10.1016/j.rser. 2019.02.032.

ASHRAE, (2005) «2005 ASHRAE HANDBOOK FUNDAMENTALS I-P Edition Supported by ASHRAE Research».

Assari M. R., Basirat Tabrizi H., y Movahedi M. J., (2018) «Experimental study on destruction of thermal stratification tank in solar collector performance», *Journal of Energy Storage*, vol. 15, pp. 124-132, feb. 2018, doi: 10.1016/j.est.2017.11. 004.

Barrantes, T. M. C. (2021). Diseño de un sistema aerotérmico para optimizar la refrigeración y el calentamiento de agua sanitaria en el centro de prácticas pre clínico y clínico de Estomatología de la Universidad Señor de Sipan.

Beckman A. W. *et. al*, (2006) «Solar Engineering of
Thermal Processes 3rd Edition 2006».

Belessiotis V. y Delyannis E., (2011) «Solar drying», *Solar Energy*, vol. 85, n.º 8, pp. 1665-1691, ago. 2011, doi: 10.1016/j.solener.2009.10.001.

Beltrán Rodríguez L., Alexandri Rionda R., Herrera Romero J., y Ojeda Galicia O., (2016) «Balance Nacional de Energía», *Secretaría de Energía, Subsecretaría de Planeación y Transición Energética. México.*, pp. 15-20.

ISSN 2523-2881

Bouhal T., Fertahi S., Agrouaz Y., El Rhafiki T., Kousksou T., y Jamil A., (2017) «Numerical modeling and optimization of thermal stratification in solar hot water storage tanks for domestic applications: CFD study», *Solar Energy*, vol. 157, n.º August, pp. 441-455, doi: 10.1016/j.solener.2017. 08.061.

Braun J. E. y Mitchell J. C., (1983) «Solar Radiation Monitoring Laboratory», *Solar Energy*, vol. 31, n.º 5, pp. 439-444.

Camayo, B., Quispe, M., Condezo, D., Massipe, J., Galarza, J. y Mucha, E. (2021). Diseño autónomo del sistema solar térmico para la deshidratación indirecta de Aguaymanto (Physalis Peruviana L.), Junín. La Granja: Revista de Ciencias de la Vida. Vol. 33(1):115-124. http://doi.org/10.17163/lgr. n33.2021.10

Castillo-Téllez M., Pilatowsky-Figueroa I., López-Vidaña E. C., Sarracino-Martínez O., y Hernández-Galvez G., (2017) «Dehydration of the red chilli (Capsicum annuum L., costeño) using an indirect-type forced convection solar dryer», *Applied Thermal Engineering*, vol. 114, pp. 1137-1144, mar. 2017, doi: 10.1016/j.applthermaleng.2016.08.114.

Cisneros, R. C. A., Menéndez, P. A., Moralobo, P. M., Trinchet, S. F., & Fernández-Aballi, A. C. (2021). Evaluación técnico-económica preliminar de la producción de electricidad a partir de plantas termosolares en Cuba/Preliminary economic and technical evaluation of the production of electricity from solar thermal plants in Cuba. *Ingeniería Energética*, *42*(1).

Comisión Nacional para el Uso Eficiente de la Energía (CONUEE), (2018) «Energía Solar Térmica Para Procesos Industriales En México»

Chira Rodríguez, A. N., Cárdenas Correa, C. A., Ma San Gómez, F. J., Seminario Gastelo, J. M., & Luna Seminario, V. A. (2020). Comparativa entre sistemas de captación solar para el diseño y análisis de un sistema de acondicionamiento para un piso de oficinas. Universidad de Piura

De Juana Sardón J. M., (1997) «Radiación y Atmósfera», pp. 95-98. Consultado: 20 de mayo de 2021 de https://www.divulgameteo.es/uploads/Radiaci%C3%B3n-Atm%C3%B3sfera.pdf

Dev S. R. S. y Raghavan V. G. S., (2012) «Advancements in Drying Techniques for Food, Fiber, and Fuel», *Drying Technology*, vol. 30, n.º 11-12, pp. 1147-1159, sep. 2012, doi: 10.1080/07373937.2012.692747.

Dincer I. y Rosen M., (2011) *Thermal Energy Storage Systems and Applications*. 2011.

Dragsted J., Furbo S., Dannemand M., y Bava F., (2017) «Thermal stratification built up in hot water tank with different inlet stratifiers», *Solar Energy*, vol. 147, pp. 414-425, doi: 10.1016/j. solener.2017.03.008.

Durán E. M., Godfrin J. C., (2004) «Aprovechamiento de la Energía Solar en la Argentina y en el Mundo», *Aprovechamiento de la Energía Solar en la Argentina y en el Mundo. Boletin energético.*, vol. 16, p. 44

Ed-Dîn Fertahi S., Bouhal T., Kousksou T., Jamil A., y Benbassou A., (2018) «Experimental study and CFD thermal assessment of horizontal hot water storage tank integrating Evacuated Tube Collectors with heat pipes», *Solar Energy*, vol. 170, pp. 234-251, ago. 2018, doi: 10.1016/j.solener.2018.05.062.

Ed-Dîn Fertahi S., Jamil A., y Benbassou A.(2018) «Review on Solar Thermal Stratified Storage Tanks (STSST): Insight on stratification studies and efficiency indicators», *Solar Energy*, vol. 176, pp. 126-145, dic. 2018, doi: 10.1016/j.solener.2018.10.028.

Ekechukwu O. V. & Norton B., (1997) «Experimental studies of integral-type natural-circulation solar-energy tropical crop dryers», *Energy Conversion and Management*, vol. 38, n.º 14, pp. 1483-1500, sep. 1997, doi: 10.1016/S0196-8904(96)00102-1.

Ekechukwu O. V. y Norton B., (1999) «Review of solar-energy drying systems II: an overview of solar drying technology», *Energy Conversion and Management*, vol. 40, n.º 6, pp. 615-655, abr. 1999, doi: 10.1016/S0196-8904(98)00093-4.

El-Sebaii A. A. y Shalaby S. M., (2012) «Solar drying of agricultural products: A review», *Renewable and Sustainable Energy Reviews*, vol. 16, n.º 1, pp. 37-43, ene. 2012, doi: 10.1016/j.rser.2011.07.134.

ISSN 2523-2881

Erdemir D., Atesoglu H., y Altuntop N., (2019) «Experimental investigation on enhancement of thermal performance with obstacle placing in the horizontal hot water tank used in solar domestic hot water system», *Renewable Energy*, vol. 138, pp. 187-197, ago. 2019, doi: 10.1016/j.renene.2019.01.075.

Esper A. y Mühlbauer W., (1998) «Solar drying - an effective means of food preservation», *Renewable Energy*, vol. 15, n.º 1, pp. 95-100, sep. 1998, doi: 10.1016/S0960-1481(98)00143-8.

Fan J. y Furbo S., (2012) «Buoyancy driven flow in a hot water tank due to standby heat loss», *Solar Energy*, doi: 10.1016/j.solener.2012.07.024.

Fan J. y Furbo S., (2012) «Thermal stratification in a hot water tank established by heat loss from the tank», *Solar Energy*, vol. 86, n.º 11, pp. 3460-3469, doi: 10.1016/j.solener .2012.07.026.

Fan J., Furbo S., y Yue H., (2015) «Development of a Hot Water Tank Simulation Program with Improved Prediction of Thermal Stratification in the Tank», *Energy Procedia*, vol. 70, pp. 193-202, doi: 10.1016/j.egypro. 2015.02.115.

FAO, (2011) «"Energy-smart" food for people and climate», 2011. http://www.fao.org/docrep/014/i2454e/i2454e00.pdf (accedido nov. 03, 2018).

FAO, (2015) «Pérdidas y desperdicios de alimentos en américa latina y el caribe», Accedido: nov. 03, 2018. [En línea]. Disponible en: http://www.fao .org/3/a-i4655s.pdf.

Farjana S. H., Huda N., Mahmud M. A. P., y Saidur R., (2018) «Solar process heat in industrial systems – A global review», *Renewable and Sustainable Energy Reviews*, vol. 82, pp. 2270-2286, feb. 2018, doi: 10.1016/j.rser. 2017.08.065.

Fertahi S. Ed D., Jamil A., y Benbassou A., (2018) «Review on Solar Thermal Stratified Storage Tanks (STSST): Insight on stratification studies and efficiency indicators», *Solar Energy*, vol. 176, n.º May, pp. 126-145, doi: 10.1016/j.solener.2018.10.028.

García O. y Pilatowsky F. I., (2017) *Aplicaciones térmicas de la energía solar*, FORDECyT - UNAM.

García, V.O., Pilatowsky, F.I., Ortíz, R.N. y Menchaca, V.C. (2019). Solar thermal dehydrating plant for agricultural products installed in Zacatecas, México. *WEENTECH Proc. Energy*, pp 1-19. Doi: 10.32438/EPE.1119

García, V.O., Pilatowsky, F.I., Ortíz, R.N. y Menchaca, V.C. (2020). Solar thermal dehydrating plant for agricultural products. Part 1: Direct air heating system. *Renew. Energy*, vol. 148, pp 1302-1320. Doi: 10.1016/j.renene.2019.10.069

Hauer A., «Evaluation of adsorbent materials for heat pump and thermal energy storage applications in open systems», 2007, doi: 10.1007/s10450-007-9054-0.

Hernández J., Escobar I., y Castilla N., (2001) «La radiación solar en invernaderos mediterráneos revista», *Horticultura*, vol. 157, pp. 1-9.

Hollick J. C., (1999) «Commercial scale solar drying», *Renewable Energy*, vol. 16, n.º 1, pp. 714-719, ene. 1999, doi: 10.1016/S0960-1481(98)00258-4.

Huang H. *et al.*, (2018) «An experimental investigation on thermal stratification characteristics with PCMs in solar water tank», *Solar Energy*, vol. 177, n.º June 2018, pp. 8-21, 2019, doi: 10.1016/j.solener.2018.11.004.

Jangam S. V., (2011) «An Overview of Recent Developments and Some R&D Challenges Related to Drying of Foods», *Drying Technology*, vol. 29, n.º 12, pp. 1343-1357, sep. 2011, doi: 10.1080/07373937.2011.594378.

Jani D. B., Mishra M., y Sahoo P. K., (2018) «A critical review on application of solar energy as renewable regeneration heat source in solid desiccant – vapor compression hybrid cooling system», *Journal of Building Engineering*, vol. 18, pp. 107-124, doi: 10.1016/j.jobe. 2018.03.012.

ISSN 2523-2881

Johane H. B. B. y Miguel L. B. L., (2015) «Análisis de las irreversibilidades en colectores solares de placas planas no isotérmicos para calentamiento de aire utilizando un modelo adimensional», *Ingeniería, Investigación y Tecnología*, vol. 14, n.º 2, pp. 237-247, doi: 10.1016/ s1405-7743(13)72239-x.

Jones L. A., Muhlfeld C. C., y Hauer F. R., (2017) «Temperature», en *Methods in Stream Ecology: Third Edition*.

Karale S. R., (2013) «A review paper on Solar Dryer», *International Journal of Engineering Research and*, vol. 3, n.º 2, p. 7, 2013.

Kumar L., Hasanuzzaman M., y Rahim N. A., (2019) «Global advancement of solar thermal energy technologies for industrial process heat and its future prospects: A review», *Energy Conversion and Management*, vol. 195, pp. 885-908, sep. 2019, doi: 10.1016/j.enconman.2019.05.081.

Kumar M. y Khatak P., (2016) «Progress in solar dryers for drying various commodities», *Renewable and Sustainable Energy Reviews*, vol. 55, pp. 346-360, mar. 2016, doi: 10.1016/j.rser.2015.10.158.

Kurşun B., (2018) «Thermal stratification enhancement in cylindrical and rectangular hot water tanks with truncated cone and pyramid shaped insulation geometry», *Solar Energy*, vol. 169, n.º May, pp. 512-525, doi: 10.1016/j.solener.2018.05.019.

Li A., Cao F., Zhang W., Shi B., y Li H., (2018) «Effects of different thermal storage tank structures on temperature stratification and thermal efficiency during charging», *Solar Energy*, vol. 173, n.º May, pp. 882-892, doi: 10.1016/j.solener.2018.08.025.

Lizana M. F. J., (2017) «Caracterización de materiales de almacenamiento de energía térmica para aplicaciones en edificación», pp. 621-637.

Mar C. E., (2015), «La Energía Solar Termoeléctrica en España La energía solar termoeléctrica en España», n.º February

Marchena Quinde, H. H., Vicente Vásquez, J. W., & Núñez Pintado, L. F. (2021). *Diseño de un Secador de Café Mediante Colectores Solares para el Distrito de la Coipa, San Ignacio, Cajamarca*. Universidad Nacional de Jaén.

Martínez P., (2002) «Funding would prevent waste of research time», *Nature*, vol. 408, n.º 6812, pp. 514-514, doi: 10.1038/35046274.

Masanet E., Masanet E., Worrell E., Graus W., y Galitsky C., (2008) «Energy Efficiency Improvement and Cost Saving Opportunities for the Fruit and Vegetable Processing Industry. An ENERGY STAR Guide for Energy and Plant Managers», LBNL-59289-Revision, 927884, ene. 2008. doi: 10.2172/927884.

Méndez R. L. I. (2016) «Caracterización de tres captadores solares planos de aire en serie y estimación de la energía proporcionada por el arreglo de captadores en Zacatecas». Tesis Licenciatura U.A.Z.

Mujumdar A. S., (2015), *Handbook of industrial drying*. Boca Raton, Florida, USA: CRC Press.

Nahle Sabag N., (2011) «Radiación Solar en la Capa exterior de la Atmósfera Terrestre y sobre la Superficie Terrestre (Suelo y Océano)», *Biology Cabinet*.

Nandwani S. (2005), «Energía solar. Conceptos básicos y su utilización», *Universidad Nacional, Heredia (Costa Rica). Jun*, pp. 1-26.

Ortíz, R.N., García, V.O., Pilatowsky, F.I., y Menchaca, V.C. (2020). Solar-LP gas hybrid plant for dehydration of food. *Appl. Therm. Eng., vol. 177,* doi: 10.1016/j.applthermaleng.2020. 115496

Ortíz, R.N., Marin, C. J.F., González, A.L., y García, V.O., (2021). Drying kinetics of natural rubber sheets under two solar termal drying systems. Renew. Energy, vol. 165, pp. 438-454. Doi: 10.1016/j.renene. 2020.11.035

Othman M. Y. H., Sopian K., Yatim B., y Daud W. R. W., (2006) «Development of advanced solar assisted drying systems», *Renewable Energy*, vol. 31, n.º 5, pp. 703-709, abr. 2006, doi: 10.1016/j.renene.2005.09.004.

ISSN 2523-2881

Pandey K. M. y Chaurasiya R., (2017) «A review on analysis and development of solar flat plate collector», *Renewable and Sustainable Energy Reviews*, vol. 67, pp. 641-650, doi: 10.1016/j.rser.2016.09.078.

Phadke P. C., Walke P. V., y Kriplani V. M., (2015) «A REVIEW ON INDIRECT SOLAR DRYERS», vol. 10, n.º 8, p. 12.

Pirasteh G., Saidur R., Rahman S. M. A., y Rahim N. A., (2014) «A review on development of solar drying applications», *Renewable and Sustainable Energy Reviews*, vol. 31, pp. 133-148, mar. 2014, doi: 10.1016/ j.rser.2013.11.052.

Rosas L. M. A., Fontes C. F. B., De Miranda Mousinho M. C. A., y Torres E. A., (2019) «Solar Photovoltaic Distributed Generation in Brazil: The Case of Resolution 482/2012», *Energy Procedia*, vol. 159, pp. 484-490, doi: 10.1016/j.egypro.2018. 12.036.

Sabbah R., Kizilel R., Selman J. R., y Al-Hallaj S., (2008) «Active (air-cooled) vs. passive (phase change material) thermal management of high power lithium-ion packs: Limitation of temperature rise and uniformity of temperature distribution», *Journal of Power Sources*, doi: 10.1016/j. jpowsour.2008.03.082.

Sardeshpande V. y Pillai I. R., (2012) «Effect of micro-level and macro-level factors on adoption potential of solar concentrators for medium temperature thermal applications», *Energy for Sustainable Development*, vol. 16, n.º 2, pp. 216-223, doi: 10.1016/j.esd.2012.01.001.

Sarı A. y Kaygusuz K., (2002) «Thermal and heat transfer characteristics in a latent heat storage system using lauric acid», *Energy Conversion and Management*, doi: 10.1016/S0196-8904(01)00187-X.

Sharma A. K., Sharma C., Mullick S. C., y Kandpal T. C., (2017) «Solar industrial process heating: A review», *Renewable and Sustainable Energy Reviews*, vol. 78, pp. 124-137, oct. 2017, doi:10.1016/j.rser.2017.04. 079.

Sharma A., Chen C. R., y Vu Lan N., (2009) «Solar-energy drying systems: A review», *Renewable and Sustainable Energy Reviews*, vol. 13, n.º 6-7, pp. 1185-1210, 2009, doi: 10.1016/j.rser.2008.08.015.

Shukla R., Sumathy K., Erickson P., y Gong J., (2013) «Recent advances in the solar water heating systems: A review», *Renewable and Sustainable Energy Reviews*. doi: 10.1016/j.rser. 2012.10.048.

Sun T. y Teja A. S., (2003) «Density, viscosity, and thermal conductivity of aqueous ethylene, diethylene, and triethylene glycol mixtures between 290 K and 450 K», *Journal of Chemical and Engineering Data*, doi: 10.1021/je025610o.

Sun T. y Teja A. S., (2004) «Density, viscosity and thermal conductivity of aqueous solutions of propylene glycol, dipropylene glycol, and tripropylene glycol between 290 K and 460 K», *Journal of Chemical and Engineering Data*, 2004, doi: 10.1021/je049960h.

Thirugnanasambandam M., Iniyan S., y Goic R., (2010) «A review of solar thermal technologies», *Renewable and Sustainable Energy Reviews*, vol. 14, n.º 1, pp. 312-322, doi: 10.1016/j.rser.2009.07.014.

Tian Y. y Zhao C. Y., (2013), «A review of solar collectors and thermal energy storage in solar thermal applications», *Applied Energy*, vol. 104, pp. 538-553, doi: 10.1016/j.apenergy.2012.11.051.

Vijaya Venkata Raman S., Iniyan S., y Goic R., (2012) «A review of solar drying technologies», *Renewable and Sustainable Energy Reviews*, vol. 16, n.º 5, pp. 2652-2670, jun. 2012, doi: 10.1016/j.rser.2012.01.007.

Wang Z., Zhang H., Huang H., Dou B., Huang X., y Goula M. A., (2019) «The experimental investigation of the thermal stratification in a solar hot water tank», *Renewable Energy*, pp. 862-874, doi: 10.1016/j.renene.2018. 11.088.

Zhao P. *et al.*, (2015) «Cryogenic power generation system recovering LNG's cryogenic energy and generating power for energy and CO_2 emission savings», *Energy*, doi: 10.1016/j. energy.2015.09.020.

ISSN 2523-2881